Characterization of Nanofluids Using Multifractal Analysis of a Liquid Droplet Trace

Jakub Augustyniak
Bialystok University of Technology
Izabela Zgłobicka
Bialystok University of Technology
Krzysztof Jan Kurzydłowski
Bialystok University of Technology
Paweł Misiak
University of Bialystok
Agnieszka Zofia Wilczewska
University of Bialystok
Jürgen Gluch
Fraunhofer Institute for Ceramic Technologies and Systems IKTS
Zhongquan Liao
Fraunhofer Institute for Ceramic Technologies and Systems IKTS
Dariusz Mariusz Perkowski (d.perkowski@pb.edu.pl)
Bialystok University of Technology

Research Article

Keywords: nanoliquid, multifractal analysis, MADLS, SEM, TEM, zeta potential, contact angle, singularity spectrum, nanoparticles

Posted Date: December 6th, 2021

DOI: https://doi.org/10.21203/rs.3.rs-1123985/v1

Abstract

This paper presents a novel approach to the analysis of nanofluids by using a nonlinear multifractal algorithm. Multifractal analysis allows to present detailed local descriptions of complex scaling behavior using a spectrum of singularity exponents. Nanoliquids prepared from nanoparticles of SiO2 (~0,01g) suspended in 100 ml of demineralized water and in 100 ml of 99,5% isopropanol were subjected to classical methods of analysis: determination of the contact angle, determination of the zeta potential, pH, and examination with a particle size analyzer. The obtained results show that the obtained nanofluid is stable and well prepared, while further nonlinear analyzes show that the usage of multifractal analysis for nanofluids can significantly improve both the process of analyzing this issue as well as its preparation, based on the multifractional spectrum.

Introduction

Fluid mechanics plays an extremely important role in many areas of industry, life and science. A serious challenge that the current world is facing is improving the quality of fluids, resulting in creating nanofluids - fluids with suspended nanoparticles. However, the preparation process of this type of fluid can be challenging (agglomeration is a major problem in nanofluid synthesis [1]) and even more so, the process allowing to verify the quality of the obtained nanofluid. The main methods by which nanoliquids are produced are the two-step method or one-step method. The two-step methoh has been widely described in publications [2], [3]. Work [4] and [5] describe the one-step method. Futhermore one can also find nanofluids prepared with deionized water, distilled water, ethylene glycol, ethylene glycol / water etc. in various concentrations [6], [7]. The stability of the nanoliquids is very important for practical reasons. The stability of nanoliquids is strongly dependent on the properties of the suspended particles and base fluid, such as particle morphology, the chemical structure of particles, and alkaline fluid [8]. The visualization of the particles within a liquid may be difficult to implement from a technical point of view (scale, number of particles, liquid, 3D spaces). In the works [9], [10] several methods recommended for the analysis of nanoparticles can be found. Nevertheless, the assessment of the quality of nanoparticles can be carried out taking into account disintegration of the particles into smaller pieces via sonication as well as evaporation process of a nanofluid droplet. Authors in [11] also mention the change of pH values of the suspension, by usage of surface activator. These and other treatments reflect the possible preparation procedures and enable the fabrication of a final product with a defined size range of particles uniformly suspended in the fluid. It must be noted that the analysis of images of samples that have undergone the evaporation process (analysis of the trace left by nanopowder) also provides information about the nature of the fluid itself (vortices inside the fluid) as well as the nature of the powder. The formation of the pattern of nanoparticles of isodensity water-based nanofluid drops has already been the subject of investigations (see [12]). Authors report two different patterns which depend on the evaporation: an o-ring and a continuous nanoparticle flower pattern. The attempt of understanding the effect of the dynamic of fluid and particle motion that allows obtaining various patterns of nanoparticle sessile after evaporation

of fluid has been presented in [13]. The three competitive, convective mechanisms have been considered. Based on obtained results, two major patterns have been identified: the o-ring and the petal-like pattern.

Further investigations in this subject [14] included the effect of nanoparticle size on evaporation and dryout characteristics of nanofluid droplets via the usage of a microfabricated linear heater array. The three main periods occurring in the evaporation process have been noticed: (i) liquid dominant evaporation, (ii) dryout progress, and (iii) formation of nanoparticle stains.

Another type of research that is gaining importance in the field of research is devoted to the nonlinear analysis of nanoliquids or their properties, such as: formulating of aggregates, convective heat transfer, critical heat flux, and subcooled pool boiling heat transfer - this research is based on fractal analysis. In the work [15] authors introduce three novel fractal models which have a good agreement between fractal model predictions and experimental data. Authors of [16] conducted experiments on the aggregate fractal dimensions and thermal conduction in nanofluids. The usage of fractals gave them information that as aggregates grow the viscosity increases at a faster rate than thermal conductivity making highly aggregated nanofluids unfavorable. On the other hand, in the paper [17] authors classified the complex stream patterns taking into consideration fractal dimensions.

In this publication we present characterization results of dried nanofluid droplets. SiO_2 nanoparticles were dispersed in water or isopropanol using sonication. Afterward, single drops were left to evaporate on the stubs to conduct microscope observations. The obtained scanning electron microscope (SEM) images were subjected to nonlinear multifractal analysis which allowed validation of the quality of the prepared nanofluid considering the size and distribution of the nanoparticles. An additional advantage of this work is the use of nonlinear multifractal analysis to attempt to characterize the quality of prepared nanoliquids based on their evaporated droplet samples.

Results

Classic approach and results As can be seen from the results presented in Tab. 1, the angles measured on each of the drops in relation to the obstruction (left angle - right angle) do not differ significantly, which proves that the conducted measurements were carried out correctly. However, it is worth mentioning the difference in the values obtained for fluids with the addition of silica nanoparticles. In both cases (water or isopropanol), the contact angle is lower than the value for pure liquids by an average of 2°, which indicates a change in the fluid viscosity, and hence lower ductility of the tested fluid. It is worth mentioning that the measurements of the wettability angle were made on carbon tape.

Table 1
Compilation of the contact angle for two samples: *A* and *B*.

Angle/specimen	sample *A*	water	sample *B*	isopropanol
Left average angle	63.49°±1°	66.68°±1°	147.67°±1°	151.81°±1°
Right average angle	63.88°±1°	67.02°±1°	147.05°±1°	151.15°±1°

The zeta potential values shown in Tab. 2 for both water and isopropanol suspensions are about -60 mV, which indicates high stability and no aggregation in time [18]. This is also confirmed by the lack of change in particle size over a month. It is worth mentioning that the submicron particles suspended in water are smaller than those in isopropanol by about 30-40 nm in terms of mean hydrodynamic diameter and are 185.9 and 212.6 nm, respectively, after a month.

Table 2
Zeta potential of silica suspensions and hydrodynamic diameter of particles in time.

medium	ζ potential	Size from MADLS		
	[mV]	[d, nm]		
		after 24 h	after a week	after a month
water	-60.89 ± 3.93	187.8 ± 7.7	186.4 ± 4.9	185.9 ± 2.5
isopropanol	-57.29 ± 1.83	221.6 ± 2.5	219.6 ± 3.6	212.6 ± 5.2

Proposed multifractal approach The results of the multifractal analysis folded as consecutive singularity spectra in one plot, for both samples, are presented in Figure 1.

In addition, the values of three characteristic points from the spectra of singularities and the dimension characterizing the width of the multifractal spectrum, which indicates the complexity of the observed process/image have been listed in Table 3.

Table 3
Summary of the most important values obtained based on multifractal analysis.

Sample / method	Mean h_{min} value	Mean h_{max} value	Mean h_0 value	Mean h_{max}-h_{min} value
A / LtR	1.575	2.719	1.986	1.143
B / LtR	1.618	2.646	1.989	1.028
A / UtD	1.661	2.765	2.048	1.104
B / UtD	1.591	2.444	1.917	0.852

The figures representing the spectra of singularities for successively taken SEM images for each sample, several characteristic features can be observed (see Figure 1). Namely, the multifractal spectra for sample *A* (Figure 1a, 1b) are arranged close to each other, even overlapping. Their h_{min}, h_{max} and h_0 values do not differ significantly from each other in the direction of UtD and LtR, which suggests correctly distributed nanopowder particles within the liquid throughout the whole sample. In the case of Figures 1c and 1d, presenting spectra for sample *B*, significant changes between the shape and position of individual curves can be noticed. This suggests that the fluid was not fully prepared properly. Thus, there is a significant

variation in the size of the observed nanopowder particles and their unregulated distribution on the sample surface.

The numerical values presented in Table 3, allow concluding that: the lower the h_{min} value, the smaller the nanopowder particles can be observed (better disintegration of the agglomerates during the sonication process), while the higher the h_{max} value, the more uniform distribution of nanopowder particles in the observed area (no agglomerates). Thus, the value of h_0 characterizes the fluid as a whole (as the sum of the particle size and their distribution in it). Therefore, the greater the value in relation to h_{min} and h_{max}, the better the nanofluid is prepared. Additionally, the width of the multifractal spectrum indicates the complexity of the tested fluid, the higher value corresponds to more uniform nanofluid (smaller nanopowder particles, more evenly distributed on the surface of the sample).

Discussion

Results for a standard approach to characterization of nanofluids Photograph showing sample *A* (Fig. 3) allow noticing a characteristic ring on the edge of the sample resembling the o-ring like pattern presented in [13], while sample B (Fig. 4) does not have such a strongly visible edge (it is visible but is irregular and disappears in places), indicating a different character the evaporation process.

The SEM imaging for both samples has been done at a magnification of 25 000 (Scios 2, ThermoFisher, USA). Exemplary images are shown in Figure 5.

Taking a closer look on the SEM images one can notice that sample *A* (Fig. 5a) and *B*

(Fig. 5b) show considerable similarities - both of them show a layer of nanoparticles, more uniform in sample A. Higher magnifications show that sample *A* contains smaller differences in the distribution of nanoparticles - assessed based on the differences in height, which in turn reflects into the sharpness of the image - difficulties in uniform focus over the entire area can be noticed. Whatmore sample *A* shows homogeneity in terms of particle size, whereas in sample *B* individual nanoparticles located on larger "flakes" (agglomerates) can be observed. Sample *B* shows voids within layers, which are not observed in sample *A*. The size of the particles in the TEM images allow us to say that the particles are below 100 nm.

When analyzing the data presented both in charts and in tables (Figure 6 and 7), two parameters are the most important. Measured particle size (Diam) and the percent of particles below that micron size (Q%). The first statement concerns the liquid immediately after the sonication process in an ultrasonic cleaner. It can be seen here that the results obtained indicate silica particles smaller than 0.709 μm - Q% at the level of 98%. The graph also shows numerous particles that were below 0.05 μm in size. The second listing is for the same fluid that was left for 24h to determine the stability of the resulting fluid with respect to the formation of agglomerates. The results are shown except for the maximum value. After 24 hours in the liquid, it can be seen that the value of the silica size for Q% at the level of 98% increased to the value of 0.727 μm, which suggests the formation of small agglomerates. The other measured powder

sizes are at a similar level which in turn suggests that the resulting fluid is stable. According to what was presented in [19], a stable nanofluid is theoretically possible as long as particles stay small enough (~100 nm).

The pH values for both samples were: 5.2 pH for sample *A* and 4.4 pH for sample *B*. According [20] to the higher the pH value the better the stability of the nanofluid. Whatmore the zeta potential also should be greater for higher pH values.

Zeta potential (ZP) is the potential at the sliding border, i.e., at the point of contact between the solid and the electrolyte solution. The ZP determines the stability and the possibility of aggregation of nanoparticles (NPs), which may be crucial for further applications. The values can be both positive and negative and are expressed in mV. Higher absolute values of the zeta potential are associated with a more stable nanofluid, it is assumed that NPs are stable above +30 mV or below -30 mV and aggregation occurs in the range from -5 to +5 mV [21]. Table 2 shows the development of the zeta potential of silica suspensions and hydrodynamic diameter of particles over time.

The DLS study showed that the second population can be observed in the spectra of silica in water after 24 hours, a week, and a month, and in isopropanol after 24 hours. It accounts for about 1% of the total, and its size is twice the size of the particles. In addition, the strongly negative value of the zeta potential suggests that these are agglomerates resulting from the process of their production, and not the process of preparing suspensions. Additionally, the DLS analyses carried out with the use of horizontal and vertical polarizers made it possible to state that the suspended silica particles are spherical, as evidenced by the overlapping of spectra recorded for both polarizers, which was presented on Figure 8.

Proposition of a new method for the characterization of nanofluids The images analyzed with the nonlinear algorithm were mainly based on moving the seen area (ROI – Region Of Interest) over the entire area of the sample in two schemes: from the left to the right edge of the sample (marked as LtR-left to right) and from top to bottom of the sample (labeled as UtD-up to down) – Figure 2. Based on obtained images, it was possible to determine the quality of the obtained fluid by analyzing the surface of the sample.

The three characteristic points, in Figure 11, have been marked with symbols: "cross", "*circle*" and "*square*". The first and third symbols refer to changes taking place in the system, depending on the point of observation, respectively locally or globally in scale. These points were determined using the polynomial approximation method (average value R^2 = 0.98 for all samples - this proves a very good adjustment of the curve to the results and could be the basis for further analysis). The maximum value in the spectrum, marked with a circle, determines the sum of two other points and identifies the entire process (h_0) [22]. The proposed approach allows to determine singularity spectrum for a single image so the method will be applied to analyze a certain selected area of each sample.

Conclusion

The nanoliquids are used in more and more applications, in various areas of life and industrial sectors. Hence, the evaluation of the preparation process and the quality of the fluids obtained is of key importance. The presented approach of the analysis of fluids with nanopowder allows to determine the degree of disintegration of the nanoparticle's agglomerates, their distribution within the sample and the complexity of the obtained nanofluid.

The samples obtained as a result of evaporation resemble those reported in the literature, while the presented tests require additional trials and analyzes to further describe both the nanofluid preparation process as well as the samples of dried droplets.

In the multifractal diagram, three characteristic points can be determined, the leftmost one in the case of nanoliquids characterizes the size of the particles suspended in the fluid - the lower the value of h_{min}, the smaller the particles appear. The rightmost point describes the distribution of nanoparticles on the surface. The greater the value of h_{max}, the better the homogenization of the fluid. The maximum value of the multifractal spectrum characterizes the repeatability of the relations found in the entire sample.

The addition of silica powder reduced the wettability of the fluid in both water and isopropanol. The silica increased the fluid density compared to the base fluid, which can be seen from the contact angle values.

Materials And Methods

Materials

To prepare nanoliquids the SiO_2 nanoparticles (~0.01g) have been suspended in 100 mL of demineralized water (HYDROLAB HLP 5sp, HYDROLAB, Poland) and in 100 ml of 99.5% isopropanol, marked sample *A* and sample *B*, respectively. Sample *A* has been sonicated in common mode, whereas sample *B* in degas mode using Ultrasonic Cleaner (ZX-615FTS, Shanghai ZX Trading Co, LTD, Shanghai) for 60 minutes according to [23]. Both samples have been sonicated without heating, at 95% power of the device (342 W ultrasonic power).

Experimental techniques

Classic approach The transmission electron microscopy (TEM) has been used to conduct visualization of silica nanopowder using a scanning TEM (Carl Zeiss Libra 200 MC Cs, Carl Zeiss AG, Oberkochen, Germany), operating at an accelerating voltage of 200 kV (see Figure 10).

Both nanoliquids were analyzed by classical methods: determination of the contact angle, determination of the zeta potential, pH, and examination with a particle size analyzer. Summing up, this work focuses mainly on two of the five parameters characterizing nanoliquids according to [24]: particle and colloidal properties.

The contact angle was measured by a Ossila Contact Angle Goniometer (United Kingdom) and differs for, see figure below (Tab. 1).

Contact angle analyses were performed by the sessile drop technique at room temperature and atmospheric pressure. Ten independent measurements for nanofluids (water and nanosilica, isopropanol and nanosilica) and five independent measurements for pure water and isopropanol were performed for each sample, each with a 15 µL water drop, and the obtained results were averaged to reduce the impact of surface nonuniformity.

The size of silica particles after the sonication process in an ultrasonic cleaner was measured by Nano Particle Size Analyzer SALD-7500nano for the water and silica solution in two stages: 1) immediately after the preparation of the liquid, and 2) 24 hours after the preparation of the liquid see Figure 6 and 7.

Another way to determine the quality of the obtained nanofluid is to determine the zeta potential and to measure the particle size by Multiangle Dynamic Light Scattering (MADLS) and Dynamic Light Scattering (DLS). Zeta potential, MADLS and DLS with horizontal or vertical polarizer were carried out using a Zetasizer Ultra (Malvern Panalytical Ltd., Malvern, UK) equipped with a 10mW helium/neon laser (λ= 633 nm) at 25 °C. The instrument settings were optimized automatically using the ZS XPLORER software (Malvern Panalytical Ltd., Malvern, UK). MADLS measurements were performed after 24 hours, a week, and a month after suspension. The particle sizes are expressed as the mean hydrodynamic diameter of 5 measurements.

The nanoparticles of Aerosil A200 from the water (sample *A*) or isopropanol (sample *B*) suspension were spread over a double-sided adhesive carbon tape on an aluminum pin disc using an automatic pipette Eppendorf Research (volume of the drop: 2 µl). The evaporation process took place at room temperature for 24 hours. For imaging at the highest resolution via scanning electron microscopy (FE-SEM) samples were coated with 10 nm of Au using a high-vacuum sputter coater (Compact Coating Unit CCU-010, Safematic, Switzerland). The imaging was carried out with a dual-beam FIB-SEM tool (Scios 2, ThermoFisher, USA) using detectors of secondary electrons: ETD and upper in-lens detector – T2, acceleration voltage of 10 kV for the electrons, 3 mm and 7 mm working distance. Figures 3b and 4b present photos of exemplary SEM pin stubs showing the evaporation effect (which took place without additional heating–free evaporation conditions) on the shape of the dried nanofluid. The magnification of the edges is presented via SEM images in Figure 3d and 4d, respectively (~100 x).

A new approach with the use of multifractals The multifractal approach opens possibilities for the visualization of materials as a heterogeneous system with all aspects as subsets of the fundamental elements. The result of this analysis presents a multifractal spectrum that describes the dimension of a fractal subset of function points. To obtain an adaptive form of division both in time and space, the result of which is the spectre of singularities, the Legendre transformation ($\tau(q)$) is used. This transformation defines the relationship between itself and the global spectrum of singularities $D(h)$ [25]:

$$D(h) = qh(q) - \tau(q), \quad (1)$$

$$h(q) = \frac{d\tau(q)}{dq}, \quad (2)$$

where: $h(q)$ is the global distribution of the Hölder exponent defined for the moment q. Negative values of q emphasize weak exponents, while positive values emphasize strong exponents. The spectrum itself can be written as:

$$D(h) = \lim_{l \to 0} \frac{\sum_{i=1}^{N(l)} \mu_i(q,l) \ln\left[\mu_i(q,l)\right]}{\ln l}, \qquad (3)$$

where $f(\alpha(q))$ is the function of moments q, $\mu_i(q,l)$ is a normalized measure as q^{th} moment of mass probability $P_i(l)$ where to estimate multifractal properties over a small interval of scales a constant range of l is taken advantage of [26]:

$$\mu_i(q,l) = \frac{P_i^q(l)}{\sum_{i=1}^{N(l)} P_i^q(l)}. \qquad (4)$$

The explementary result of the multifractal analysis algorithm of SEM images in the form of a singularity spectrum for sample A is shown in Figure 9.

The polynomial approximation method allows to determine three characteristic points on the graph (see Figure 11).

Declarations

Aknowlegments

Project financed by the program of the Poland Ministry of Science and Higher Education “Regional Initiative of Excellence” (years 2019-2022). Project number 011/RID/2019/19. The authors are grateful to Adrian Dubicki, for the sample images made on Tagarno microskop.

AUTHOR CONTRIBUTIONS

Augustyniak J. proposed the concept of multifractal approach to characterize nanoliquids. Misiak P., Wilczewska A. Z. performer the processing of the nanofluid using MADLS; Jürgen Gluch, Zhongquan Liao performed the TEM images of the samples; Zgłobicka I performed the SEM and contact angle measurements, Augustyniak J. and Perkowski D. M performed: the preparation of the nanofluid, the multifractral analysis, necessary calculations as well as preparing the paper. Perkowski D. M and Kurzydłowski K. supervised the project. All authors contributed to the general discussion, revision and editing the manuscript.

DECLARATION OF COMPERING INTEREST

The authors declare that they have no conflict of interest.

References

[1] X. Q. Wang and A. S. Mujumdar, “A review on nanofluids - Part II: Experiments and applications,” *Brazilian Journal of Chemical Engineering*. 2008, doi: 10.1590/S0104-66322008000400002.

[2] L. Jia, Y. Chen, S. Lei, S. Mo, Z. Liu, and X. Shao, “Effect of magnetic field and surfactant on dispersion of Graphene/water nanofluid during solidification,” in *Energy Procedia*, 2014, doi: 10.1016/j.egypro.2014.12.124.

[3] W. Duangthongsuk and S. Wongwises, “Measurement of temperature-dependent thermal conductivity and viscosity of TiO2-water nanofluids,” *Exp. Therm. Fluid Sci.*, 2009, doi: 10.1016/j.expthermflusci.2009.01.005.

[4] P. Hajiani and F. Larachi, “Magnetic-field assisted mixing of liquids using magnetic nanoparticles,” *Chem. Eng. Process. Process Intensif.*, 2014, doi: 10.1016/j.cep.2014.03.012.

[5] S. U. S. Choi, W. Yu, J. R. Hull, Z. G. Zhang, and F. E. Lockwood, “Nanofluids for vehicle thermal management,” in *SAE Technical Papers*, 2001, doi: 10.4271/2001-01-1706.

[6] M. S. Liu, M. Ching-Cheng Lin, I. Te Huang, and C. C. Wang, “Enhancement of thermal conductivity with carbon nanotube for nanofluids,” *Int. Commun. Heat Mass Transf.*, 2005, doi: 10.1016/j.icheatmasstransfer.2005.05.005.

[7] X. F. Li, D. S. Zhu, X. J. Wang, N. Wang, J. W. Gao, and H. Li, “Thermal conductivity enhancement dependent pH and chemical surfactant for Cu-H2O nanofluids,” *Thermochim. Acta*, 2008, doi: 10.1016/j.tca.2008.01.008.

[8] Y. Hwang *et al.*, “Stability and thermal conductivity characteristics of nanofluids,” *Thermochim. Acta*, 2007, doi: 10.1016/j.tca.2006.11.036.

[9] A. W. Salamon, “The current world of nanomaterial characterization: Discussion of analytical instruments for nanomaterial characterization,” *Environmental Engineering Science*. 2013, doi: 10.1089/ees.2012.0330.

[10] LINSINGER Thomas; ROEBBEN Gert; et al., “Requirements on measurements for the implementation of the European Commission definition of the term ‘nanomaterial,’” *Publ. Off. Eur. Union*, 2013, doi: 10.2787/63995.

[11] Y. Xuan and Q. Li, “Heat transfer enhancement of nanofluids,” *Int. J. Heat Fluid Flow*, 2000, doi: 10.1016/S0142-727X(99)00067-3.

[12] D. Brutin, “Influence of relative humidity and nano-particle concentration on pattern formation and evaporation rate of pinned drying drops of nanofluids,” *Colloids Surfaces A Physicochem. Eng. Asp.*, 2013, doi: 10.1016/j.colsurfa.2013.03.012.

[13] X. Zhong, A. Crivoi, and F. Duan, “Sessile nanofluid droplet drying,” *Advances in Colloid and Interface Science*. 2015, doi: 10.1016/j.cis.2014.12.003.

[14] H. C. Chan, S. Paik, J. B. Tipton, and K. D. Kihm, “Effect of nanoparticle sizes and number densities on the evaporation and dryout characteristics for strongly pinned nanofluid droplets,” *Langmuir*, 2007, doi: 10.1021/la061661y.

[15] J. Cai, X. Hu, B. Xiao, Y. Zhou, and W. Wei, “Recent developments on fractal-based approaches to nanofluids and nanoparticle aggregation,” *International Journal of Heat and Mass Transfer*. 2017, doi: 10.1016/j.ijheatmasstransfer.2016.10.011.

[16] P. E. Gharagozloo and K. E. Goodson, “Aggregate fractal dimensions and thermal conduction in nanofluids,” *J. Appl. Phys.*, 2010, doi: 10.1063/1.3481423.

[17] Y. Lv *et al.*, “Fractal Analysis of Positive Streamer Patterns in Transformer Oil-Based TiO2 Nanofluid,” *IEEE Trans. Plasma Sci.*, 2017, doi: 10.1109/TPS.2017.2705167.

[18] A. Kumar and C. K. Dixit, “Methods for characterization of nanoparticles,” in *Advances in Nanomedicine for the Delivery of Therapeutic Nucleic Acids*, 2017.

[19] E. A. Hauser, “The history of colloid science,” *Journal of Chemical Education*. 1955, doi: 10.1021/ed032p2.

[20] X. J. Wang, X. Li, and S. Yang, “Influence of pH and SDBS on the stability and thermal conductivity of nanofluids,” *Energy and Fuels*, 2009, doi: 10.1021/ef800865a.

[21] S. Nimesh, R. Chandra, and N. Gupta, *Advances in Nanomedicine for the Delivery of Therapeutic Nucleic Acids*. 2017.

[22] J. Augustyniak and D. M. Perkowski, “Compound analysis of gas bubble trajectories with help of multifractal algorithm,” *Exp. Therm. Fluid Sci.*, 2021, doi: 10.1016/j.expthermflusci.2021.110351.

[23] A. Asadi and I. M. Alarifi, “Effects of ultrasonication time on stability, dynamic viscosity, and pumping power management of MWCNT-water nanofluid: an experimental study,” *Sci. Rep.*, 2020, doi: 10.1038/s41598-020-71978-9.

[24] D. K. Devendiran and V. A. Amirtham, “A review on preparation, characterization, properties and applications of nanofluids,” *Renewable and Sustainable Energy Reviews*. 2016, doi: 10.1016/j.rser.2016.01.055.

[25] J. F. Muzy, E. Bacry, and A. Arneodo, “Multifractal formalism for fractal signals: The structure-function approach versus the wavelet-transform modulus-maxima method,” *Phys. Rev. E*, vol. 47, no. 2, pp. 875–884, 1993, doi: 10.1103/PhysRevE.47.875.

[26] B. Yao, F. Imani, A. S. Sakpal, E. W. Reutzel, and H. Yang, “Multifractal Analysis of Image Profiles for the Characterization and Detection of Defects in Additive Manufacturing,” *J. Manuf. Sci. Eng. Trans. ASME*, 2018, doi: 10.1115/1.4037891.

Figures

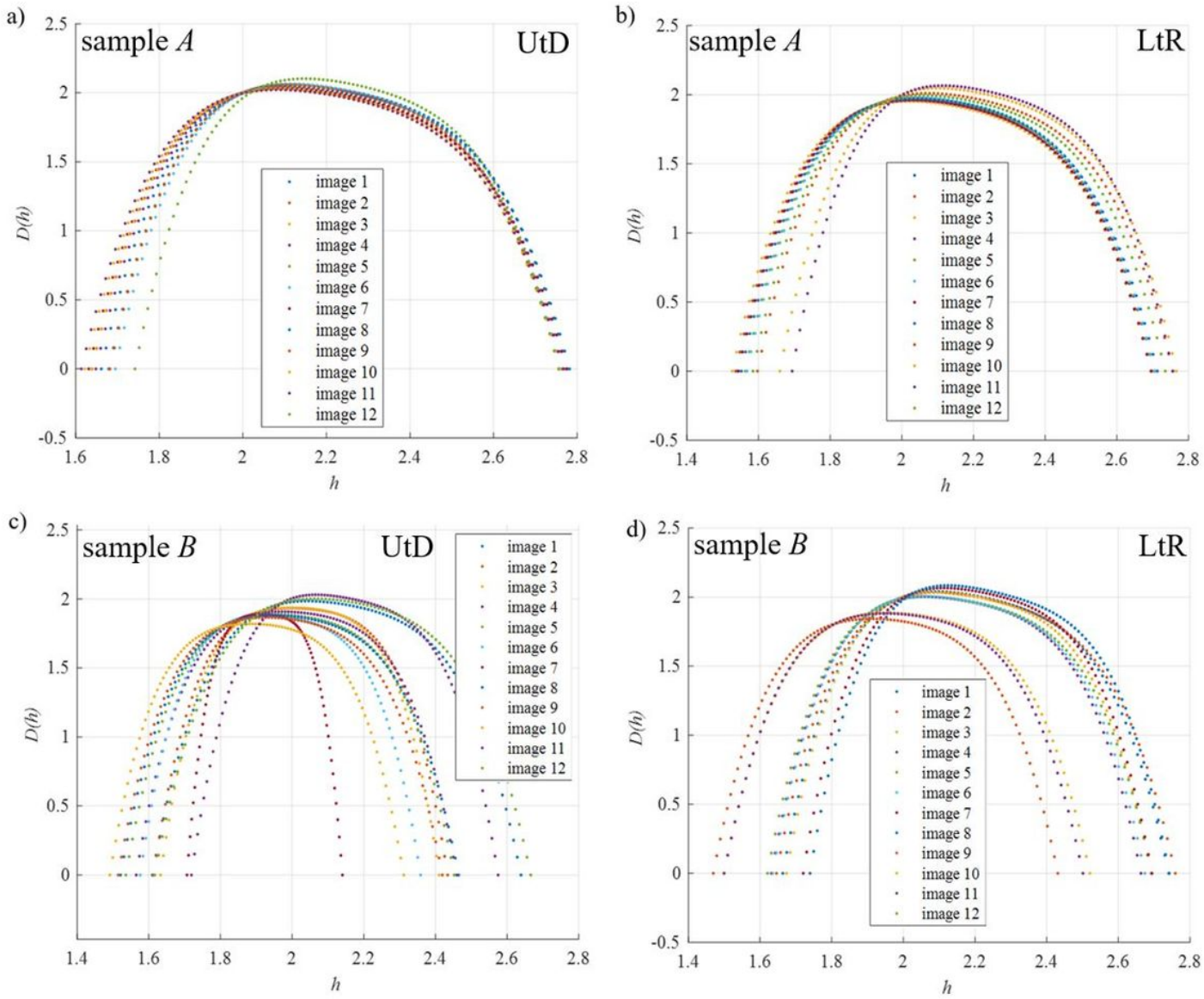

Figure 1

Singularity spectra obtained for sample A: a) the direction of the UtD images; b) direction of the LtR images and sample B: c) direction of the UtD images; d) direction of the LtR images.

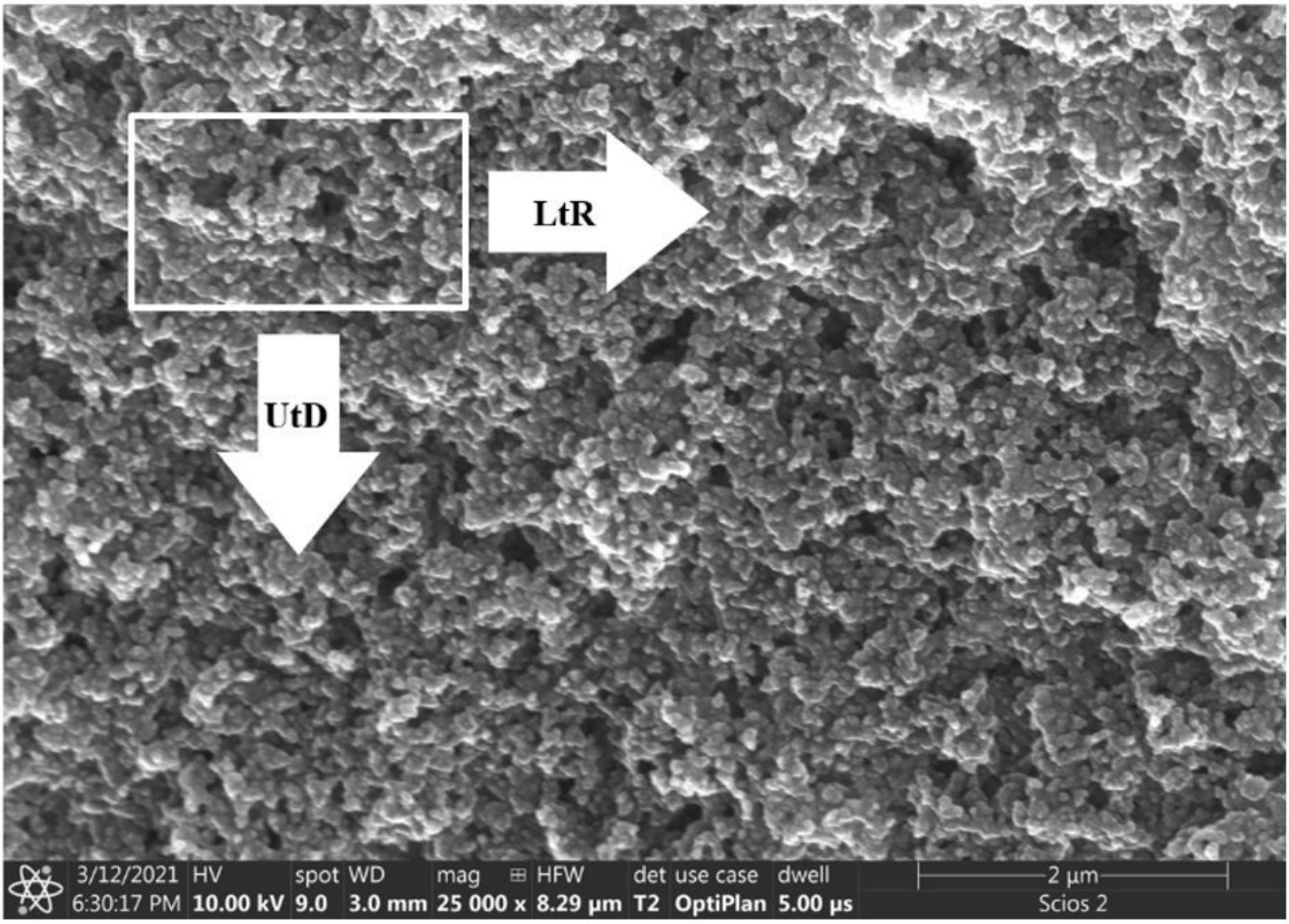

Figure 2

Scheme of the imaging process during SEM observations (sample B).

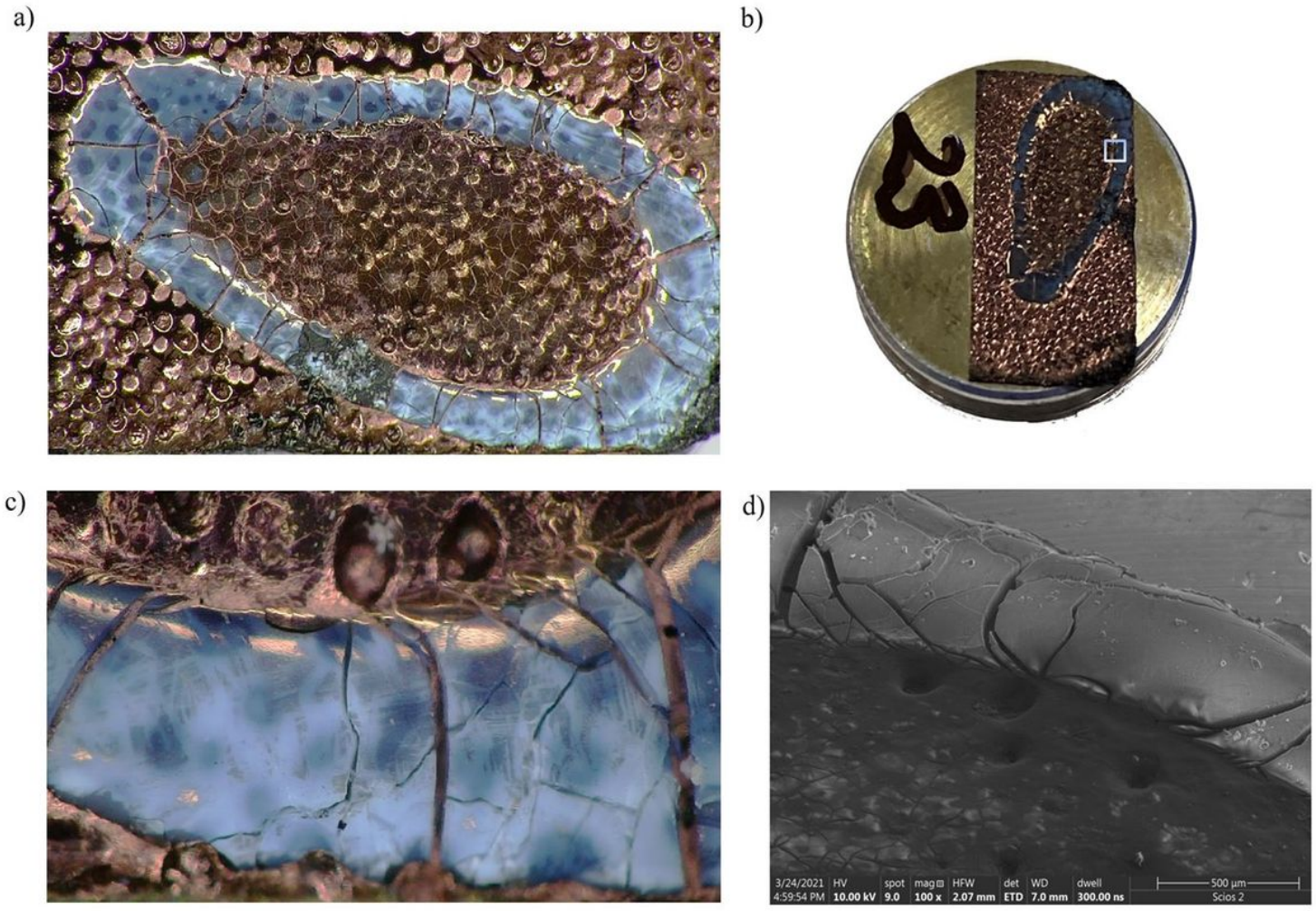

Figure 3

Photos of sample A: a) image from optical microscopy; b) macro image of the pin; c) image from optical microscopy of the marked area; d) SEM images of the edge of the sample – powder particles were found both on the edge and inside.

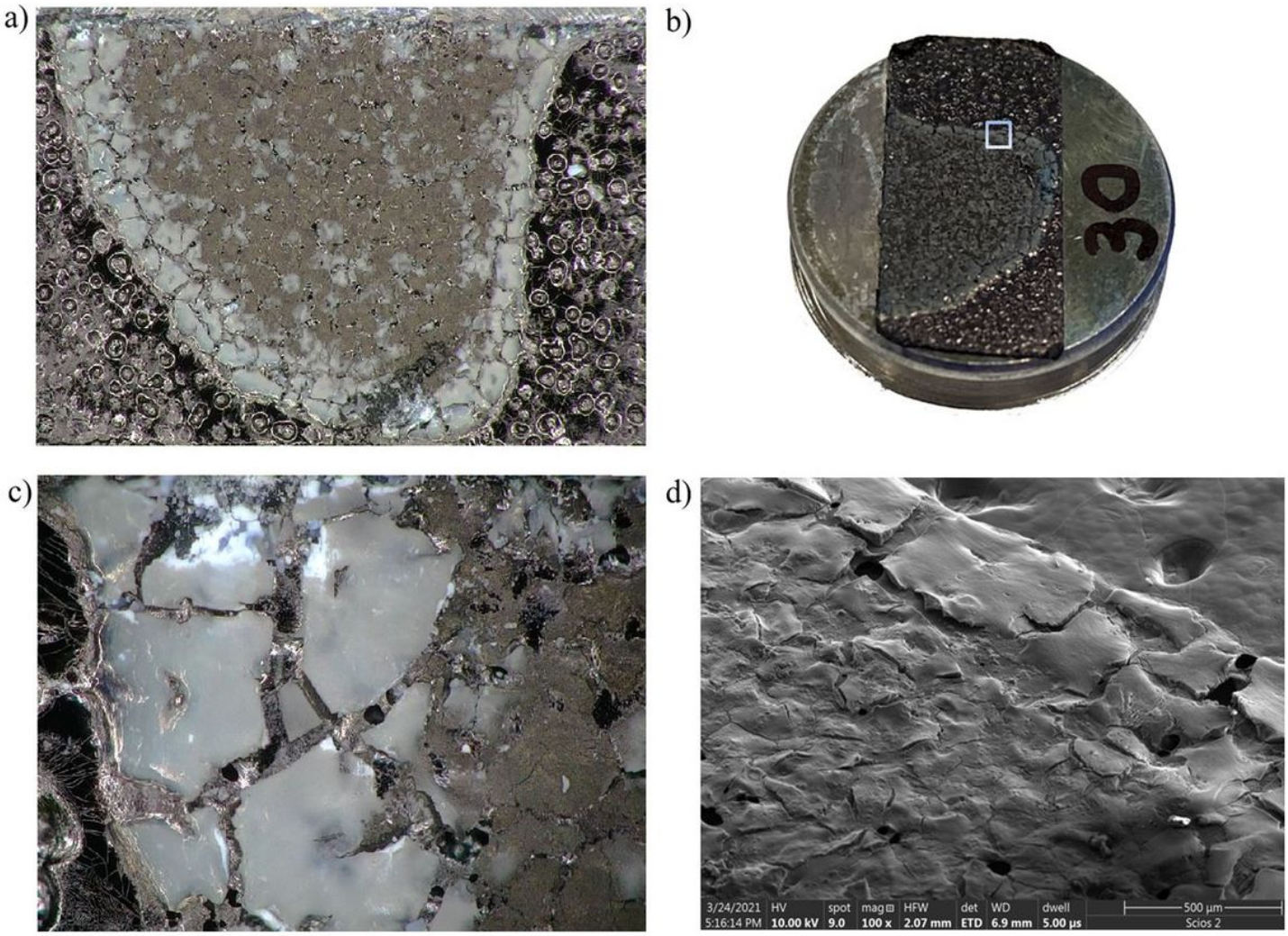

Figure 4

Photos of sample B: a) image from optical microscopy; b) macro image of the pin; c) image from optical microscopy of the marked area; d) SEM images of the edge of the sample – powder particles were found both on the edge and inside.

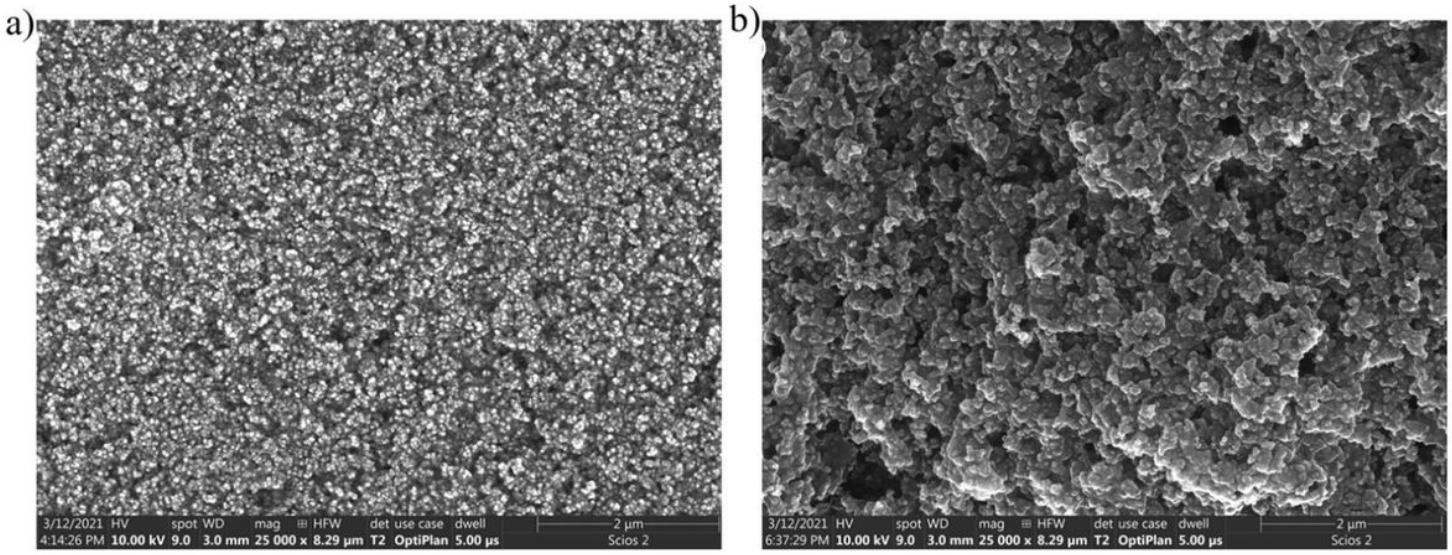

Figure 5

SEM images of a) sample A; b) sample B.

Figure 6

Silica particle size distribution for the sample water + SiO2 immediately after the preparation of the liquid.

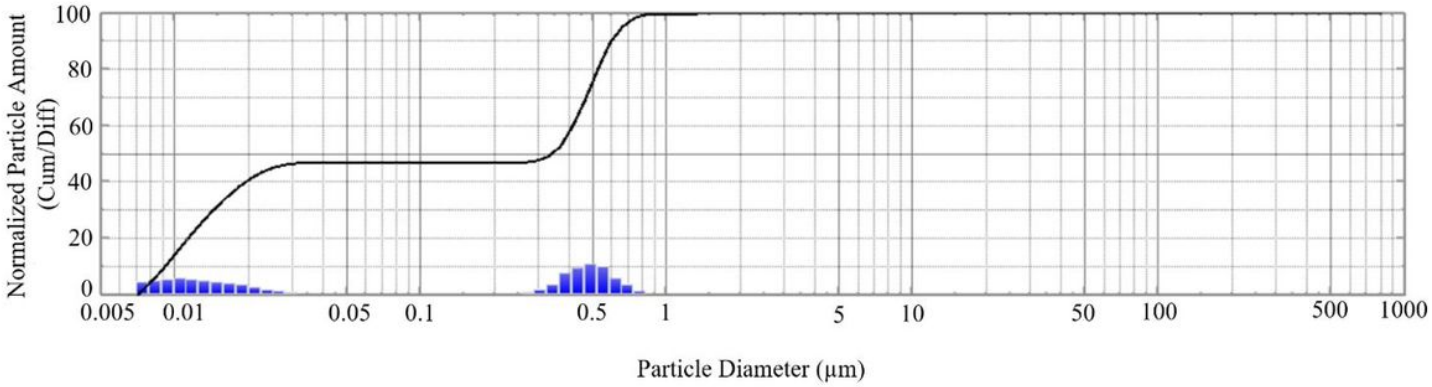

	Cum% Q(%)	Diam x(µm)		Cum% Q(%)	Diam x(µm)		Cum% Q(%)	Diam x(µm)		Cum% Q(%)	Diam x(µm)
1	98.0	0.727	14	72.0	0.478	27	46.0	0.027	40	20.0	0.011
2	96.0	0.690	15	70.0	0.467	28	44.0	0.023	41	18.0	0.011
3	94.0	0.655	16	68.0	0.455	29	42.0	0.021	42	16.0	0.010
4	92.0	0.622	17	66.0	0.443	30	40.0	0.019	43	14.0	0.010
5	90.0	0.590	18	64.0	0.430	31	38.0	0.018	44	12.0	0.009
6	88.0	0.574	19	62.0	0.418	32	36.0	0.017	45	10.0	0.009
7	86.0	0.561	20	60.0	0.407	33	34.0	0.016	46	8.0	0.009
8	84.0	0.548	21	58.0	0.396	34	32.0	0.015	47	6.0	0.008
9	82.0	0.536	22	56.0	0.385	35	30.0	0.014	48	4.0	0.008
10	80.0	0.524	23	54.0	0.374	36	28.0	0.014	49	2.0	0.007
11	78.0	0.512	24	52.0	0.356	37	26.0	0.013			
12	76.0	0.500	25	50.0	0.325	38	24.0	0.012			
13	74.0	0.489	26	48.0	0.296	39	22.0	0.012			

Figure 7

Silica particle size distribution for the sample water + SiO2 24 hours after the preparation of the liquid.

Figure 8

Particle size spectra recorded with MADLS.

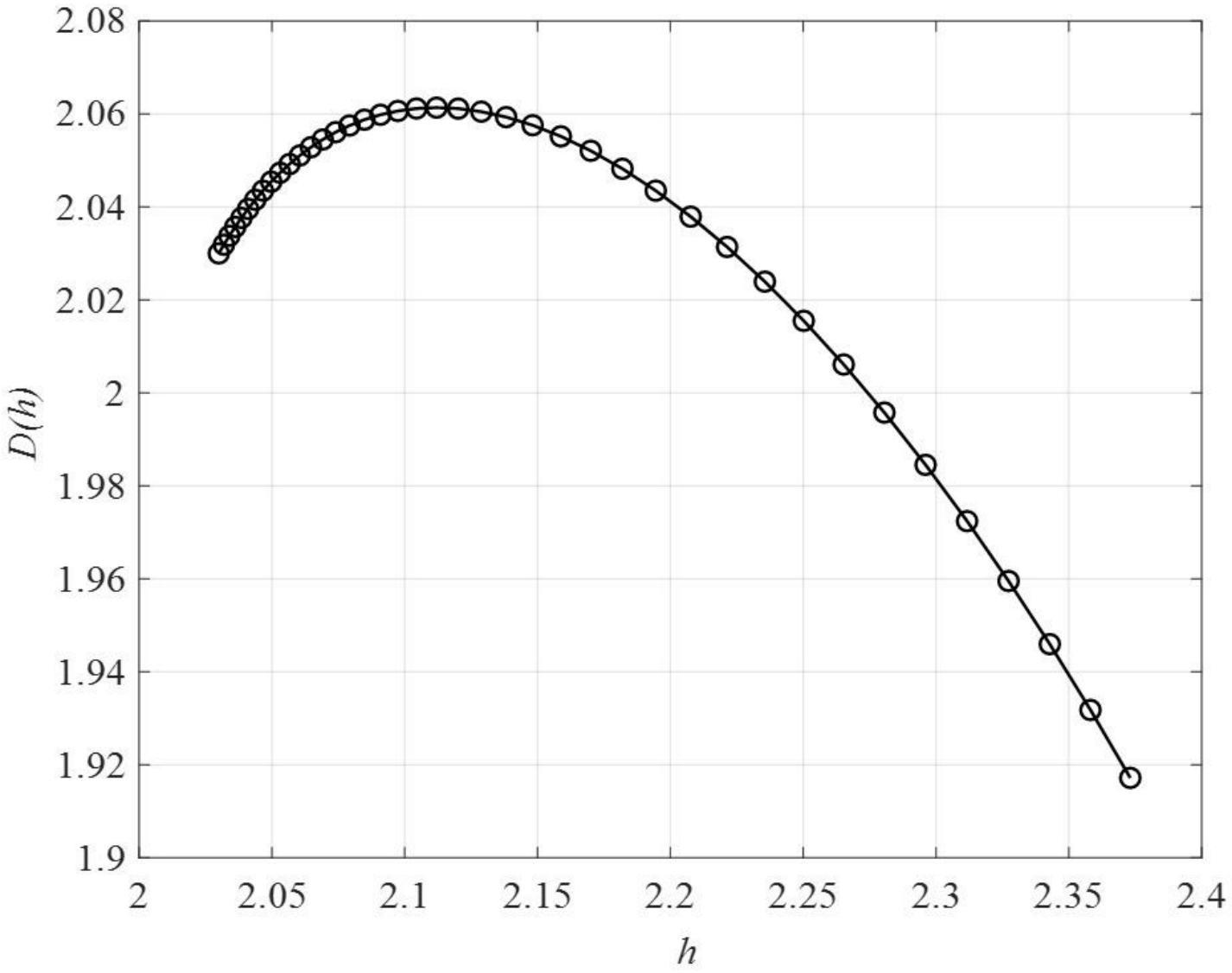

Figure 9

Example of multifractal spectrum calculated for a single SEM image (sample A).

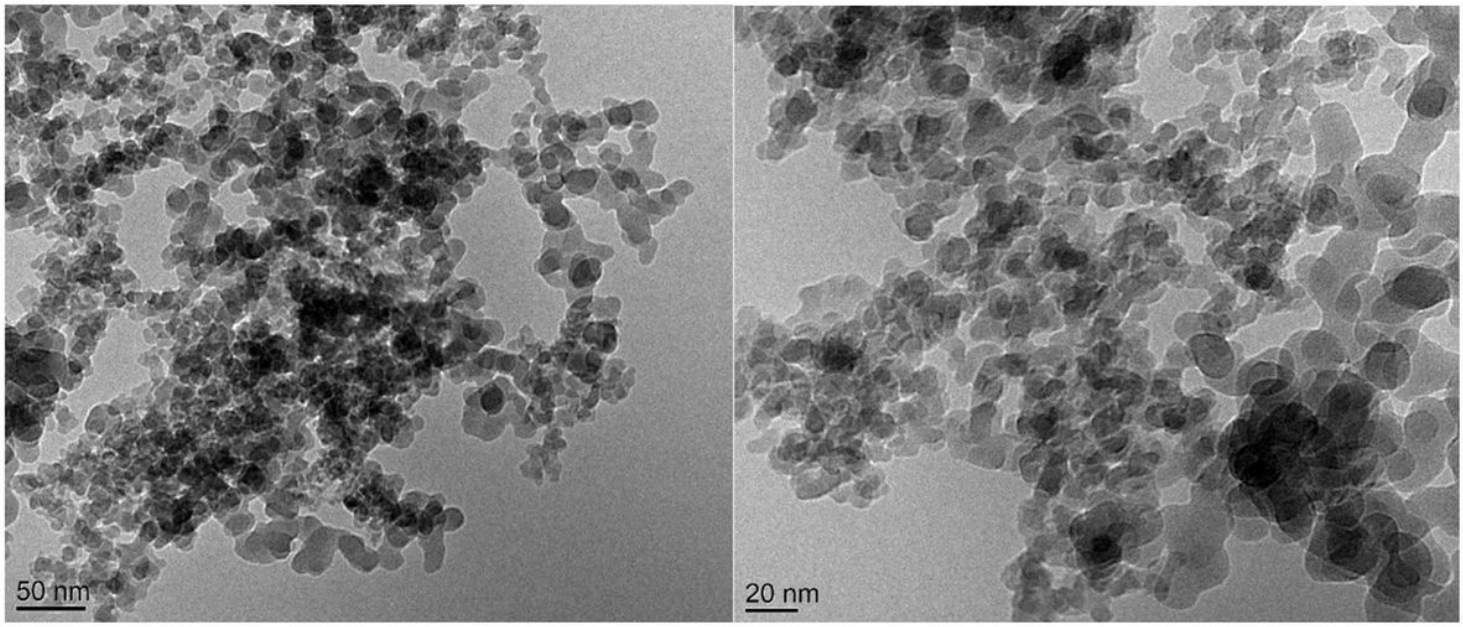

Figure 10

TEM images of raw SiO2 powder.

Figure 11

Multifractal spectrum for a single SEM image with three characteristic points: hmin, hmax and h0 (sample A).